PROCEEDINGS OF SCIENCE

Combined KM3NeT/ARCA and ANTARES searches for point-like neutrino emission

B. Caiffi,[a,*] V. Kulikovskiy,[a] S. Alves Garre,[b] J. Aublin,[c] A. Heijboer,[d] G. Illuminati,[e] R. Muller,[e] V. Parisi,[a,f] M. Sanguineti[a,f] and S. Zavatarelli[a] on behalf of the ANTARES and KM3NeT collaborations

[a] *INFN, Sezione di Genova, Via Dodecaneso 33, Genova, 16146 Italy*
[b] *IFIC - Instituto de Física Corpuscular (CSIC - Universitat de València), c/Catedrático José Beltrán, 2, 46980 Paterna, Valencia, Spain*
[c] *Université Paris Cité, CNRS, Astroparticule et Cosmologie, F-75013 Paris, France*
[d] *Nikhef, National Institute for Subatomic Physics, PO Box 41882, Amsterdam, 1009 DB Netherlands*
[e] *INFN, Sezione di Bologna, v.le C. Berti-Pichat, 6/2, Bologna, 40127 Italy*
[f] *Università di Genova, Via Dodecaneso 33, Genova, 16146 Italy*

E-mail: km3net-astro-convenor@km3net.de

Neutrino telescopes are at the forefront of high-energy astrophysics, offering unique insights into some of the most extreme and energetic phenomena in the Universe. The ANTARES detector, which operated for 16 years off the coast of Toulon (France) until 2022, has played a pioneering role in deep-sea neutrino observations. Building upon its legacy, the next-generation KM3NeT/ARCA neutrino telescope is currently under construction in the deep waters of the Mediterranean near Southern Italy, designed to push the boundaries of astrophysical neutrino detection.

In recent years, the search for astrophysical neutrino sources has gained momentum, as their detection would provide crucial evidence of hadronic acceleration mechanisms at play in the most powerful cosmic environments. This study presents an analysis of the combined dataset from ANTARES and the available KM3NeT/ARCA observations, focusing on the detection of high-energy neutrinos from both point-like sources.

A comprehensive catalog of about 100 point-like and extended astrophysical sources has been examined for potential neutrino emissions. This selection includes prominent γ-ray emitters, Galactic γ-ray sources with possible hadronic components (TeVCat), extragalactic AGNs with intense radio flux detected by VLBI, and the most promising candidates previously investigated by IceCube. The results of this analysis represent a significant step toward uncovering the origin of cosmic neutrinos and advancing multi-messenger astronomy.

39th International Cosmic Ray Conference (ICRC 2025)
14-24 July 2025
Geneva, Switzerland

[*] Speaker

PoS(ICRC2025)1002

1. Introduction

Following IceCube's key discoveries—such as the diffuse astrophysical neutrino flux [1] and the association of individual neutrinos with sources like TXS 0506+056 [2] and Messier 77 [3]—the search for their origins continues. KM3NeT/ARCA will provide a complementary view, particularly of the Galactic Plane and Center.

KM3NeT/ARCA [4], under construction off Sicily at 3500 m depth, will comprise two building blocks of 115 lines each, with 18 digital optical modules per line. Each module hosts 31 PMTs, enabling a directional resolution better than 0.2° for muon neutrinos above 10 TeV.

Its predecessor, ANTARES [5], operated from 2008 to 2022 off Toulon, France, at 2500 m depth. It consisted of 12 lines, each with 25 storeys of three 10-inch PMTs, for a total of 885 PMTs. This configuration offered optimal visibility of the Southern Sky and Galactic Center.

Both detectors rely on the detection of Cherenkov light from charged particles produced in neutrino interactions. The timing and position of detected photons allow reconstruction of neutrino direction and energy. Identifying cosmic signals within the atmospheric background requires statistical methods based on Monte Carlo simulations; the present analysis employs a binned likelihood approach.

2. Data samples for point-like and extended sources analysis

In this joint analysis, each data set refers to a distinct detector period and dedicated event selection, ensuring no event overlaps. The datasets used in this analysis include:

- ANTARES tracks/showers: events selected as tracks/showers according to the selection criteria of the ANTARES point source analysis [7];
- ARCA6 tracks: track-like events from the KM3NeT/ARCA detector with 6 detection lines (92 days) [10];
- ARCA8 tracks: track-like events from the KM3NeT/ARCA detector with 8 detection lines (212 days) [10];
- ARCA19 tracks: track-like events from the KM3NeT/ARCA detector with 19 detection lines (48.4 days) [11];
- ARCA21 tracks: track-like events from the KM3NeT/ARCA detector with 21 detection lines (287.4 days) [11].

3. Signal and background models and likelihood formalism

The compatibility of the data with a point-like or extended source hypothesis is quantified by comparing multidimensional histograms of reconstructed event parameters.

Scanning all bins across datasets is equivalent to analyzing a single bin in a combined histogram with the total number of bins from all datasets. The histogram of the observed events, N, is compared bin by bin versus a scalable estimate of the number of signal events, S, expected for a reference flux, $\Phi_{\rm ref}$, and the number of background events, B, as follows:

$$\log L = \sum_{i}^{\rm N_{bins}} N_i \log(B_i + \zeta S_i) - (B_i + \zeta S_i), \tag{1}$$

where ζ is the signal flux scale. The logarithm of the likelihood ratio is used as a test-statistic to quantify the compatibility of the data with the signal/background hypotheses and it is described as follows:

$$\lambda = \log L(\zeta = \hat{\zeta}) - \log L(\zeta = 0), \tag{2}$$

where $\hat{\zeta}$ is the fitted signal flux scale. The λ distributions are built for each true signal scaling ζ and they are used to extract limits with the Neyman approach [12]. The sensitivity is defined as the median upper limit on ζ for 90% C.L. and can be converted to the flux as $\Phi_{90} = \zeta_{90}\Phi_{\rm ref}$.

For the ARCA samples, the signal estimation S_i is computed using two-dimensional histograms as a function of the logarithm of the angular distance to the source center, α, and the logarithm of the reconstructed energy, $E_{\rm rec}$, for each source declination. To account for the declination-dependent detector efficiency, bands of width 0.2 in $\sin(\delta)$ are considered, where δ is the declination. These same histograms are also employed in the likelihood calculations for signal evaluation.

In the case of the ANTARES track sample, S_i is determined using three-dimensional histograms as a function of $\log(\alpha)$, $E_{\rm rec}$, and the angular error estimation β, again using 0.2-wide $\sin(\delta)$ bands. These 3D histograms are used consistently for both signal generation and evaluation.

For the ANTARES shower sample, S_i is calculated using two-dimensional histograms as a function of α and $E_{\rm rec}$, obtained by convolving the MC event energy distribution with the point spread function. In this case, different histograms are used for signal generation and evaluation: for generation, 0.2-wide $\sin(\delta)$ bands are applied, whereas for evaluation, the declination bands are not considered. These choices for the ANTARES sample are consistent with the methodology adopted in the official ANTARES point source analysis [7–9].

The S_i histograms are rescaled according to the expected number of events at a given declination, evaluated from finely binned histograms obtained as the product of the effective area as a function of $\sin(\delta)$ and the reference flux Φ_0=10^{-8} GeV cm^{-2} s^{-1}.

The background estimation, B_i, for the ARCA sample is computed using data-driven two-dimensional histograms as a function of α and $E_{\rm rec}$, within $\sin(\delta)$ bands of width 0.2. These same 2D histograms are also employed for background evaluation in the likelihood calculations. Specifically, the number of background events $N_{\alpha_{\rm bin},E_{\rm bin}}$ in a given bin ($\alpha_{\rm bin}$, $E_{\rm bin}$) is calculated as

$$N_{\alpha_{\rm bin},E_{\rm bin}} = \rho_\delta \cdot 2\pi\,(\cos(\alpha_{\rm bin\ min}) - \cos(\alpha_{\rm bin\ max})) \cdot \rho_E \cdot (E_{\rm bin\ max} - E_{\rm bin\ min}) \tag{3}$$

where $\rho_\delta = \frac{N_{\rm decl}}{2\pi(\sin({\rm decl}_{\rm band\ max}) - \sin({\rm decl}_{\rm band\ min}))}$ is the event density in the considered declination band, $\rho_E = \frac{N_{\rm E}}{E_{\rm bin\ max} - E_{\rm bin\ min}}$ is the event density in the considered energy bin and the other terms are geometrical/normalization factors. For all ARCA datasets except ARCA8, the declination band sizes have been enlarged (from 0.2 in $\sin(\delta)$ to 0.6 for ARCA6, 0.9 for ARCA21, and even a single band from $\sin(\delta) = -1$ to 0.8 for ARCA19) to ensure sufficient statistics across all relevant distributions.

In the case of the ANTARES track sample, the background histograms used for B_i differ between the generation (obtained from data) and evaluation (from MC). Nonetheless, both procedures are based on two-dimensional histograms as functions of β and E_{rec}, constructed within $\sin(\delta)$ bands of width 0.2. The α dimension is incorporated by weighting each α slice according to the geometrical factor, as previously described for the ARCA sample.

Similarly, for the ANTARES shower sample, the generation of the background B_i is data-driven, while the evaluation is MC–based. The two-dimensional histograms are constructed by convolving the declination distribution with the energy spectrum, following a method analogous to that used for the ARCA samples. These distinct approaches to background estimation and evaluation for the ANTARES samples have been adopted to maintain consistency with the official ANTARES point source analysis.

4. Results

The point source sensitivity and discovery fluxes as a function of declination are shown in Fig. 1 for KM3NeT/ARCA 6-21, ANTARES and joint analyses. In the current work, ANTARES contributes most significantly to the joint analyses; combining with KM3NeT/ARCA the performance improves by 20% with respect to the ANTARES standalone analysis.

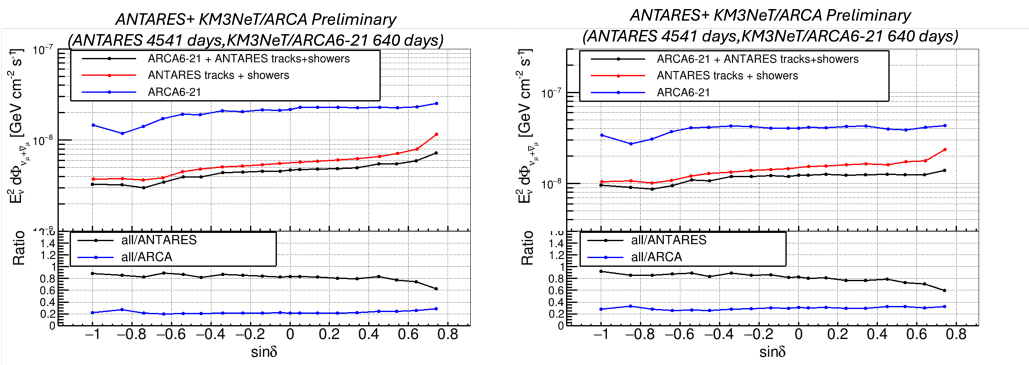

Figure 1: Left: 90% C.L. median upper limits on the one-flavour neutrino flux as a function of declination. Right: 50% 5σ discovery flux on the one-flavour neutrino flux as a function of declination.

The 90% C.L. upper limits for each source are shown in Fig. 2 for KM3NeT/ARCA+ANTARES. The results of the unblinding are summarized in Table 1. The best candidates mostly coincide with the ones from the standalone ANTARES search [7] as it is expected from the modest contribution of the ARCA samples.

The source with the lowest p-value in this analysis is MG3J225517+2409 with a pre-trial p-value of $4.0 \cdot 10^{-5} \pm 4 \cdot 10^{-6}$, obtained with $2 \cdot 10^{6}$ pseudo-experiments. This corresponds to a significance of $\sigma_{\mathrm{pre-trial}} = 3.94$ (the post-trial significance is under evaluation). Its best flux, corresponding to the best signal strenght value $\hat{\zeta}$, is $\hat{\phi} = 1.38 \cdot 10^{-8}\ \mathrm{GeV^{-1}cm^{-2}s^{-1}}$. This object was included in the candidate list as it was the most promising candidate in the ANTARES search based on Fermi 3LAC catalogue with 1255 out of 1420 objects in the field of view of ANTARES [13]. In the standalone ANTARES analysis this candidate reached a p-value of $2.4 \cdot 10^{-4}$ (3.5σ), being the most significant source among 167 candidates. The 90% C.L. upper limit flux is changed from

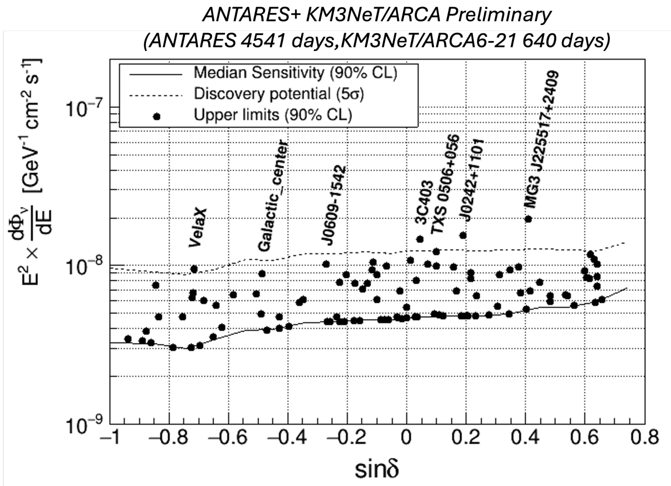

Figure 2: 90% C.L. upper limits (dots) on the one-flavour neutrino flux normalization for the investigated astrophysical candidates as a function of the source declination, assuming an $E^{-2.0}$ spectrum. The names of the sources for which a pre-trial significance greater than 2 has been obtained are reported next to the corresponding upper limits. The solid (dashed) line represents the 90% C.L. median upper limit (50% 5σ discovery flux).

$2.28 \cdot 10^{-8}\,\mathrm{GeV^{-1}cm^{-2}s^{-1}}$ (ANTARES) to $1.96 \cdot 10^{-8}\,\mathrm{GeV^{-1}cm^{-2}s^{-1}}$ (this search). In Fig.3 (left), the distribution of ANTARES and KM3NeT/ARCA events near MG3 J225517+2409 is shown in equatorial coordinates (RA, DEC). The marker opacity represents the $\log_{10}$ of the ratio between the Poisson probabilities for bin i, calculated assuming the presence of a signal at the best-fit strength ($\hat{\zeta}$), and assuming no signal ($\zeta = 0$); that is,

$$\log_{10}\left[\frac{\mathrm{Poisson}(N_i \mid B_i + \hat{\zeta} S_i)}{\mathrm{Poisson}(N_i \mid B_i)}\right].$$

An ARCA 21 event has an error box that includes the source location and contributes considerably to the combined event significance. This is indicated by its marker opacity, whose value of 1.4 corresponds to a probability of being signal-like that is 25 times higher than that of being background-like.

The second most significant candidate is J0242+1101, with a p-value of $9.2 \cdot 10^{-4} \pm 0.2 \cdot 10^{-4}$, corresponding to a pre-trial significance of $\sigma_{\mathrm{pre-trial}} = 3.12$ and an upper limit of $\phi_{90} = 1.55 \cdot 10^{-8}\,\mathrm{GeV^{-1}\,cm^{-2}\,s^{-1}}$. This source ranked fourth in the standalone ANTARES analysis, where it had a p-value of 0.0074 (2.4σ). Although the p-value has improved, the pre-trial significance remains close to 3σ. No ARCA events contribute at the signal-like level compared to the three ANTARES track events already observed (see Fig. 3, right panel).

The second most promising source in the standalone ANTARES analysis was 3C403, which showed a p-value of 0.00048 (3.3σ) [13]. It was originally selected from a sample of 65 hard X-ray radio galaxies, within which it exhibited a pre-trial p-value of 2.3×10^{-4}, corresponding to a significance of 3.7σ. In the current analysis, which combines ANTARES and ARCA datasets, however, its p-value has increased to 0.0013, more than doubling, and indicating a reduced significance. This

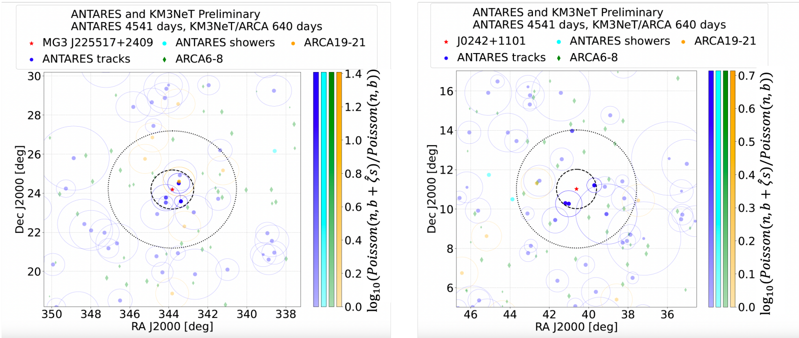

Figure 3: Distribution of the ANTARES and KM3NeT/ARCA events close to the most significant source MG3 J225517+2409 (on the left) and second-most significant source J0242+1101 (on the right) found in each search in the equatorial coordinates (RA, DEC). Error bands for events with > 2° error are not shown. The marker opacity corresponds to the contribution of this event to the observed test statistics (see text) while the marker size is scaled inversely with the number of events in the corresponding analysis bin.

trend suggests that the significance of 3C403 is diminishing as more data are incorporated and the method is refined.

The skymap with all studied candidates in this analysis is shown in Fig. 4. The sources color scale represents $\log_{10}$(p-value). For sources with $\log_{10}$(p-value) <-2, the exact p-value is also indicated.

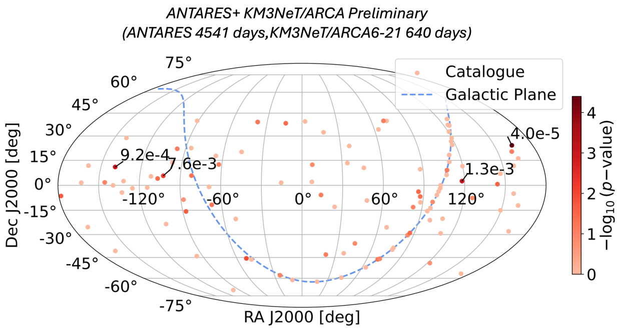

Figure 4: Skymap of the candidates, with $\log_{10}$(p-value) indicated by color. For sources with $\log_{10}(\mathrm{p-value}) < -2$, the exact p-value is also displayed next to the source.

5. Conclusions

In this contribution, we have presented the results of the combined point source analysis of KM3NeT/ARCA 6-21 and ANTARES data. Both the sensitivity and discovery potential benefit from the inclusion of the ARCA dataset, improving standalone ANTARES data analysis performance by approximately 20%.

We analysed a list of 106 candidate sources, including both point-like and extended sources with a Gaussian morphology model. The most significant sources show results in a good agreement with the ones from the ANTARES standalone analysis. The most promising source is

Name	RA [°]	δ [°]	Ext [°]	$\hat{\zeta}$	p-value	$\phi^{90\%}_{\mathrm{C.L.}}$	Name	RA [°]	δ [°]	Ext [°]	$\hat{\zeta}$	p-value	$\phi^{90\%}_{\mathrm{C.L.}}$
LMC N132D	81.2	-69.65	0.0	-	-	0.27	J0108+0135	17.16	1.58	0.0	-	-	0.17
SNR G318.2+00.1	224.42	-59.46	0.31	-	-	0.26	PKS 0215+015	34.45	1.75	0.0	0.17	0.1	0.804
IC-hotspot South hemisphere	350.2	-56.5	0.0	-	-	0.48	J1229+0203	187.28	2.05	0.0	-	-	0.405
HESS J1614-518	243.54	-51.87	0.0	-	-	0.075	TXS 0310+022	48.3	2.5	0.0	-	-	0.47
PKS 2005-489	302.37	-48.82	0.0	0.03	0.19	0.48	**3C403**	**298.07**	**2.51**	**0.0**	**0.57**	**0.0013**	**1.47**
RX J0852.0-4622	133.0	-46.37	0.63	-	-	0.3	J0433+0521	68.3	5.35	0.0	-	-	0.49
HESS J1641-463	250.26	-46.3	0.0	0.24	0.058	0.62	**TXS 0506+056**	**77.35**	**5.7**	**0.0**	**0.54**	**0.0076**	**1.2**
VelaX	**128.75**	**-45.6**	**0.58**	**0.46**	**0.01009**	**0.95**	HESS J0632+057	98.24	5.81	0.0	0.306	0.047	1.0
PKS 0537-441	84.71	-44.08	0.0	-	-	0.28	1LHAASO J1908+0615u	287.05	6.26	0.72	-	-	0.49
CentaurusA	201.36	-43.02	0.0	0.15	0.08	0.604	PKS 2145+067	327.02	6.96	0.0	-	-	0.3
PKS 1424-418	216.99	-42.11	0.0	-	-	0.307	W 49B	287.78	9.09	0.0	0.23	0.06	0.97
J0106-4034	16.69	-40.57	0.0	-	-	0.36	OT 081	267.89	9.65	0.0	-	-	0.69
RX J1713.7-3946	258.36	-39.77	0.65	-	-	0.56	PKS 1502+106	226.1	10.49	0.0	-	-	0.29
CTB 37A	258.56	-38.52	0.0	-	-	0.408	**J0242+1101**	**40.62**	**11.02**	**0.0**	**1.13**	**0.00092**	**1.6**
PKS 1454-354	224.36	-35.67	0.0	0.1	0.13	0.65	J2232+1143	338.15	11.73	0.0	-	-	0.2
HESS J1741-302	265.32	-30.38	0.0	0.096	0.14	0.7	J0121+1149	20.42	11.83	0.0	-	-	0.47
J1924-2914	291.21	-29.24	0.0	-	-	0.49	J1230+1223	187.71	12.39	0.0	0.14	0.13	0.83
Galactic center	266.42	-29.01	0.0	0.32	0.034	0.9	J0750+1231	117.72	12.52	0.0	0.29	0.085	0.9
J2258-2758	344.52	-27.97	0.0	-	-	0.25	PKS 1413+135	214.03	13.35	0.0	-	-	0.097
J1625-2527	246.45	-25.46	0.0	-	-	0.35	J0530+1331	82.74	13.53	0.0	-	-	0.65
NGC 253	11.88	-25.29	0.0	-	-	0.48	W 51	290.75	14.14	0.12	-	-	0.48
J0457-2324	74.26	-23.41	0.0	-	-	0.27	J2253+1608	343.49	16.15	0.0	-	-	0.32
J1833-210A	278.42	-21.06	0.0	-	-	0.58	PKS 0735+178	114.53	17.71	0.0	-	-	0.6
J0836-2016	129.16	-20.28	0.0	-	-	0.61	1LHAASO J1928+1813u	292.07	18.23	1.26	-	-	0.87
J1911-2006	287.79	-20.12	0.0	-	-	0.4	J0854+2006	133.7	20.11	0.0	-	-	0.42
J0609-1542	**92.42**	**-15.71**	**0.0**	**0.24**	**0.02**	**1.013**	RGB J2243+203	340.98	20.35	0.0	0.2	0.081	0.94
SNR G015.4+00.1	274.52	-15.47	0.0	-	-	0.4	Crab Nebula	83.55	22.05	0.0	0.307	0.07	0.98
J2158-1501	329.53	-15.02	0.0	-	-	0.205	IC 443	94.21	22.5	0.16	-	-	0.67
1LHAASO J1825-1337u	276.45	-13.63	0.0	-	-	0.47	PKS 1424+240	216.76	23.8	0.0	-	-	0.52
QSO 1730-130	263.3	-13.1	0.0	0.15	0.1	0.8	**MG3 J225517+2409**	**343.82**	**24.19**	**0.0**	**1.38**	**0.00004**	**1.96**
J1337-1257	204.42	-12.96	0.0	-	-	0.42	3HWC J1950+242	297.42	24.46	0.0	-	-	0.69
J2246-1206	341.58	-12.11	0.0	-	-	0.2	1LHAASO J1959+2846u	299.78	28.78	0.58	-	-	0.59
PKS 0727-11	112.58	-11.7	0.0	0.27	0.06	0.9	J0237+2848	39.47	28.8	0.0	-	-	0.65
TXS 1749-101	268.15	-10.2	0.0	-	-	0.081	J1310+3220	197.62	32.35	0.0	-	-	0.65
HESS J1828-099	277.24	-9.99	0.0	0.13	0.13	0.8	J1613+3412	243.42	34.21	0.0	-	-	0.56
J1512-0905	228.21	-9.1	0.0	-	-	0.3	1LHAASO J2018+3643u	304.65	36.72	0.48	-	-	0.93
J0607-0834	92.0	-8.58	0.0	0.021	0.19	0.708	J2015+3710	303.87	37.18	0.0	-	-	0.84
QSO 2022-077	306.4	-7.6	0.0	0.13	0.13	0.8	Mkn 421	166.11	38.21	0.0	0.49	0.034	1.16
RS Ophiuchi	267.55	-6.71	0.0	0.24	0.047	0.93	J0927+3902	141.76	39.04	0.0	0.4	0.05	1.096
J0006-0623	**1.56**	**-6.39**	**0.0**	**0.43**	**0.021**	**1.054**	NGC 4151	182.63	39.41	0.0	-	-	0.4
3C279	194.05	-5.79	0.0	0.29	0.07	0.9	Mkn 501	253.47	39.76	0.0	-	-	0.74
1LHAASO J1839-0548u	279.79	-5.81	0.44	-	-	0.6	J1642+3948	250.75	39.81	0.0	0.24	0.08	1.024
J2225-0457	336.45	-4.95	0.0	-	-	0.32	J0555+3948	88.88	39.81	0.0	-	-	0.85
4FGL J0307.8-0419	46.95	-4.33	0.0	-	-	0.36	CygOB2	307.44	41.04	2.17	-	-	0.47
PKS 1741-038	266.0	-3.83	0.0	0.37	0.034	1.0	3HWC J1951+266	297.9	26.61	1.7	-	-	0.79
1LHAASO J1843-0335u	280.91	-3.6	0.72	-	-	0.2	Westerlund 1	251.76	-45.85	0.61	0.2	0.094	0.67
J0339-0146	54.88	-1.78	0.0	-	-	0.47	Danks 1	198.12	-62.69	0.58	-	-	0.25
J0423-0120	65.82	-1.34	0.0	-	-	0.69	NGC 3603	168.79	-61.26	0.0	-	-	0.39
J0725-0054	111.46	-0.92	0.0	-	-	0.13	Westerlund 2	155.99	-57.7	0.75	0.25	0.095	0.75
1LHAASO J1848-0001u	282.19	-0.02	0.0	-	-	0.27	HESS J1848-018	281.95	-1.75	0.0	-	-	0.47
NGC 1068	40.67	-0.01	0.12	-	-	0.6	CGCG 420-015	73.35	4.06	0.0	0.28	0.037	1.021
J2136+0041	324.16	0.7	0.0	0.49	0.025	1.072	1LHAASO J1959+1129u	299.82	11.49	0.0	-	-	0.36
J1058+0133	164.62	1.57	0.0	-	-	0.42	1LHAASO J2002+3244u	300.64	32.74	0.0	-	-	0.65

Table 1: List of analyzed astrophysical objects. Reported are the source's name, equatorial coordinates (RA, δ), best-fit signal strength $\hat{\zeta}$ (i.e. signal flux scale where 1 corresponds to 10^{-8} GeV cm^{-2} s^{-1}) , pre-trial p-value, and 90% C.L. upper limits on the flux normalization factor for a $E^{-2.0}$ spectrum, $\Phi_0^{90\%}$ (in units of 10^{-8} GeV cm^{-2} s^{-1}). Sources for which a pre-trial significance greater than 2 has been obtained are highlighted in bold. Dashes (–) in the fitted signal strength and pre-trial p-value indicate sources with a null fitted signal.

MG3 J225155+2217, which yielded the lowest pre-trial p-value of 4 10^{-5} , corresponding to a significance of 3.94σ. The associated best flux is $1.38{\cdot}10^{-8}$ $\mathrm{GeV^{-1}cm^{-2}s^{-1}}$. The first KM3NeT/ARCA building block is expected to be completed in few years, indicating rapid growth for KM3NeT in the near future. As the KM3NeT/ARCA detector configuration expands and more data are collected, the ARCA contribution to this analysis will be more enhanced, especially at higher energies.

References

[1] IceCube Collaboration , Evidence for High-Energy Extraterrestrial Neutrinos at the IceCube Detector. Science 342, 1242856 (2013)

[2] The IceCube Collaboration, Multimessenger observations of a flaring blazar coincident with high-energy neutrino IceCube-170922A. Science 361, eaat1378 (2018)

[3] IceCube Collaboration, Evidence for neutrino emission from the nearby active galaxy NGC 1068, Science 378, 538–543 (2022).

[4] KM3NeT Collaboration, Letter of Intent for KM3NeT 2.0. Journal of Physics G: Nuclear and Particle Physics, 43 (8), 08400 (2016)

[5] ANTARES collaboration, ANTARES: the first undersea neutrino telescope. Nucl. Instrum. Meth. A, 656, 11-38 (2011)

[6] KM3NeT Collaboration, The KM3NeT multi-PMT optical module. JINST 17 P07038 (2022)

[7] ANTARES collaboration, The ANTARES detector: Two decades of neutrino searches in the Mediterranean Sea, Physics Reports, Volumes 1121–1124, (2025)

[8] A. Albert, et al., First all-flavor neutrino pointlike source search with the ANTARES neutrino telescope, Phys. Rev. D 96 (8) (2017) 082001.

[9] S. A. Garre, Search for the Origin of Cosmic Rays with the ANTARES Neutrino Telescope (Ph.D. thesis) Universitat de València (2025), pp. 116-127

[10] B. Caiffi et al, Search for cosmic neutrino point sources and extended sources with 6-8 lines of KM3NeT/ARCA. Poster at Neutrino 2022 conference (2022)

[11] R. Muller et al, Search for cosmic neutrino point sources and extended sources with 6-21 lines of KM3NeT/ARCA. PoS(ICRC2023) 444 (2023) 1018

[12] J. Neyman, Philosophical Transactions of the Royal Society of London. Series A, Mathematical and Physical Sciences (1937)

[13] A. Albert et al, ANTARES Search for Point Sources of Neutrinos Using Astrophysical Catalogs: A Likelihood Analysis, 2021 ApJ 911 48 DOI 10.3847/1538-4357/abe53c

Full Authors List: The KM3NeT Collaboration

O. Adriani[b,a], A. Albert[c,be], A.R. Alhebsi[d], S. Alshalloudi[d], M. Alshamsi[e], S. Alves Garre[f], F. Ameli[g], M. Andre[h], L. Aphecetche[i], M. Ardid[j], S. Ardid[j], J. Aublin[k], F. Badaracco[m,l], L. Bailly-Salins[n], B. Baret[k], A. Bariego-Quintana[f], M. Barnard[o], Y. Becherini[k], M. Bendahman[p], F. Benfenati Gualandi[r,q], M. Benhassi[s,p], D.M. Benoit[t], Z. Beňušová[v,u], E. Berbee[w], E. Berti[b], V. Bertin[e], P. Betti[b], S. Biagi[x], M. Boettcher[o], D. Bonanno[x], M. Bondì[y], S. Bottai[b], A.B. Bouasla[bf], J. Boumaaza[z], M. Bouta[e], M. Bouwhuis[w], C. Bozza[aa,p], R.M. Bozza[ab,p], H. Brânzaş[ac], F. Bretaudeau[i], M. Breuhaus[e], R. Bruijn[ad,w], J. Brunner[e], R. Bruno[y], E. Buis[w,ae], R. Buompane[s,p], I. Burriel[f], J. Busto[e], B. Caiffi[m], D. Calvo[f], A. Capone[g,af], F. Carenini[r,q], V. Carretero[ad,w], T. Cartraud[k], P. Castaldi[ag,q], V. Cecchini[f], S. Celli[g,af], L. Cerisy[e], M. Chabab[ah], A. Chen[ai], S. Cherubini[aj,x], T. Chiarusi[q], W. Chung[ak], M. Circella[al], R. Clark[am], R. Cocimano[x], J.A.B. Coelho[k], A. Coleiro[k], A. Condorelli[k], R. Coniglione[x], P. Coyle[e], A. Creusot[k], G. Cuttone[x], R. Dallier[i], A. De Benedittis[s,p], G. De Wasseige[am], V. Decoene[i], P. Deguire[e], I. Del Rosso[r,q], L.S. Di Mauro[x], I. Di Palma[g,af], A.F. Díaz[an], D. Diego-Tortosa[x], C. Distefano[x], A. Domi[ao], C. Donzaud[k], D. Dornic[e], E. Drakopoulou[ap], D. Drouhin[c,be], J.-G. Ducoin[e], P. Duverne[k], R. Dvornický[v], T. Eberl[ao], E. Eckerová[v,u], A. Eddymaoui[z], T. van Eeden[w], M. Eff[k], D. van Eijk[w], I. El Bojaddaini[aq], S. El Hedri[k], S. El Mentawi[e], V. Ellajosyula[m], A. Enzenhöfer[e], M. Farino[ak], G. Ferrara[aj,x], M. D. Filipović[ar], F. Filippini[q], D. Franciotti[x], L.A. Fusco[aa,p], T. Gal[ao], J. García Méndez[j], A. Garcia Soto[f], C. Gatius Oliver[w], N. Geißelbrecht[ao], E. Genton[am], H. Ghaddari[aq], L. Gialanella[s,p], B.K. Gibson[t], E. Giorgio[x], I. Goos[k], P. Goswami[k], S.R. Gozzini[f], R. Gracia[ao], B. Guillon[n], C. Haack[ao], C. Hanna[ak], H. van Haren[as], E. Hazelton[ak], A. Heijboer[w], L. Hennig[ao], J.J. Hernández-Rey[f], A. Idrissi[x], W. Idrissi Ibnsalih[p], G. Illuminati[q], R. Jaimes[f], O. Janik[ao], D. Joly[e], M. de Jong[at,w], P. de Jong[ad,w], B.J. Jung[w], P. Kalaczyński[bg,au], U.F. Katz[ao], J. Keegans[t], V. Kikvadze[av], G. Kistauri[aw,av], C. Kopper[ao], A. Kouchner[ax,k], Y. Y. Kovalev[ay], L. Krupa[u], V. Kueviakoe[w], V. Kulikovskiy[m], R. Kvatadze[aw], M. Labalme[n], R. Lahmann[ao], M. Lamoureux[am], A. Langella[ak], G. Larosa[x], C. Lastoria[n], J. Lazar[am], A. Lazo[f], G. Lehaut[n], V. Lemaître[am], E. Leonora[y], N. Lessing[f], G. Levi[r,q], M. Lindsey Clark[k], F. Longhitano[y], S. Madarapu[f], F. Magnani[e], L. Malerba[m,l], F. Mamedov[u], A. Manfreda[p], A. Manousakis[az], M. Marconi[l,m], A. Margiotta[r,q], A. Marinelli[ab,p], C. Markou[ap], L. Martin[i], M. Mastrodicasa[af,g], S. Mastroianni[p], J. Mauro[am], K.C.K. Mehta[au], G. Miele[ab,p], P. Migliozzi[p], E. Migneco[x], M.L. Mitsou[s,p], C.M. Mollo[p], L. Morales-Gallegos[s,p], N. Mori[b], A. Moussa[aq], I. Mozun Mateo[n], R. Muller[q], M.R. Musone[s,p], M. Musumeci[x], S. Navas[ba], A. Nayerhoda[al], C.A. Nicolau[g], B. Nkosi[ai], B. Ó Fearraigh[m], V. Oliviero[ab,p], A. Orlando[x], E. Oukacha[k], L. Pacini[b], D. Paesani[x], J. Palacios González[f], G. Papalashvili[al,av], P. Papini[b], V. Parisi[l,m], A. Parmar[n], C. Pastore[al], A. M. Păun[ac], G.E. Păvălaş[ac], S. Peña Martínez[k], M. Perrin-Terrin[e], V. Pestel[n], M. Petropavlova[u,bh], P. Piattelli[x], A. Plavin[ay,bi], C. Poirè[aa,p], V. Popa[†2ac], T. Pradier[c], J. Prado[f], S. Pulvirenti[x], C.A. Quiroz-Rangel[j], N. Randazzo[y], A. Ratnani[bb], S. Razzaque[bc], I.C. Rea[p], D. Real[f], G. Riccobene[x], J. Robinson[o], A. Romanov[l,m,n], E. Ros[ay], A. Šaina[f], F. Salesa Greus[f], D.F.E. Samtleben[at,w], A. Sánchez Losa[f], S. Sanfilippo[x], M. Sanguineti[l,m], D. Santonocito[x], P. Sapienza[x], M. Scaringella[b], M. Scarnera[am,k], J. Schnabel[ao], J. Schumann[ao], J. Seneca[w], P. A. Sevle Myhr[am], I. Sgura[al], R. Shanidze[av], Chengyu Shao[bj,e], A. Sharma[k], Y. Shitov[u], F. Šimkovic[v], A. Simonelli[p], A. Sinopoulou[y], B. Spisso[p], M. Spurio[r,q], O. Starodubtsev[b], D. Stavropoulos[ap], I. Štekl[u], D. Stocco[i], M. Taiuti[l,m], Y. Tayalati[z,bb], H. Thiersen[o], I. Tosta e Melo[y,aj], B. Trocmé[k], V. Tsourapis[ap], C. Tully[ak], E. Tzamariudaki[ap], A. Ukleja[au], A. Vacheret[n], V. Valsecchi[x], V. Van Elewyck[ax,k], G. Vannoye[l,m], E. Vannuccini[b], G. Vasileiadis[bd], F. Vazquez de Sola[w], A. Veutro[g,af], S. Viola[x], D. Vivolo[s,p], A. van Vliet[d], E. de Wolf[ad,w], I. Lhenry-Yvon[k], S. Zavatarelli[m], D. Zito[x], J.D. Zornoza[f], and J. Zúñiga[f].

[a]Università di Firenze, Dipartimento di Fisica e Astronomia, via Sansone 1, Sesto Fiorentino, 50019 Italy
[b]INFN, Sezione di Firenze, via Sansone 1, Sesto Fiorentino, 50019 Italy
[c]Université de Strasbourg, CNRS, IPHC UMR 7178, F-67000 Strasbourg, France
[d]Khalifa University of Science and Technology, Department of Physics, PO Box 127788, Abu Dhabi, United Arab Emirates
[e]Aix Marseille Univ, CNRS/IN2P3, CPPM, Marseille, France
[f]IFIC - Instituto de Física Corpuscular (CSIC - Universitat de València), c/Catedrático José Beltrán, 2, 46980 Paterna, Valencia, Spain
[g]INFN, Sezione di Roma, Piazzale Aldo Moro, 2 - c/o Dipartimento di Fisica, Edificio, G.Marconi, Roma, 00185 Italy
[h]Universitat Politècnica de Catalunya, Laboratori d'Aplicacions Bioacústiques, Centre Tecnològic de Vilanova i la Geltrú, Avda. Rambla Exposició, s/n, Vilanova i la Geltrú, 08800 Spain
[i]Subatech, IMT Atlantique, IN2P3-CNRS, Nantes Université, 4 rue Alfred Kastler - La Chantrerie, Nantes, BP 20722 44307 France
[j]Universitat Politècnica de València, Instituto de Investigación para la Gestión Integrada de las Zonas Costeras, C/ Paranimf, 1, Gandia, 46730 Spain
[k]Université Paris Cité, CNRS, Astroparticule et Cosmologie, F-75013 Paris, France
[l]Università di Genova, Via Dodecaneso 33, Genova, 16146 Italy
[m]INFN, Sezione di Genova, Via Dodecaneso 33, Genova, 16146 Italy
[n]LPC CAEN, Normandie Univ, ENSICAEN, UNICAEN, CNRS/IN2P3, 6 boulevard Maréchal Juin, Caen, 14050 France
[o]North-West University, Centre for Space Research, Private Bag X6001, Potchefstroom, 2520 South Africa
[p]INFN, Sezione di Napoli, Complesso Universitario di Monte S. Angelo, Via Cintia ed. G, Napoli, 80126 Italy
[q]INFN, Sezione di Bologna, v.le C. Berti-Pichat, 6/2, Bologna, 40127 Italy
[r]Università di Bologna, Dipartimento di Fisica e Astronomia, v.le C. Berti-Pichat, 6/2, Bologna, 40127 Italy

[2]Deceased

PoS(ICRC2025)1002

[s]Università degli Studi della Campania "Luigi Vanvitelli", Dipartimento di Matematica e Fisica, viale Lincoln 5, Caserta, 81100 Italy
[t]E. A. Milne Centre for Astrophysics, University of Hull, Hull, HU6 7RX, United Kingdom
[u]Czech Technical University in Prague, Institute of Experimental and Applied Physics, Husova 240/5, Prague, 110 00 Czech Republic
[v]Comenius University in Bratislava, Department of Nuclear Physics and Biophysics, Mlynska dolina F1, Bratislava, 842 48 Slovak Republic
[w]Nikhef, National Institute for Subatomic Physics, PO Box 41882, Amsterdam, 1009 DB Netherlands
[x]INFN, Laboratori Nazionali del Sud, (LNS) Via S. Sofia 62, Catania, 95123 Italy
[y]INFN, Sezione di Catania, (INFN-CT) Via Santa Sofia 64, Catania, 95123 Italy
[z]University Mohammed V in Rabat, Faculty of Sciences, 4 av. Ibn Battouta, B.P. 1014, R.P. 10000 Rabat, Morocco
[aa]Università di Salerno e INFN Gruppo Collegato di Salerno, Dipartimento di Fisica, Via Giovanni Paolo II 132, Fisciano, 84084 Italy
[ab]Università di Napoli “Federico II”, Dip. Scienze Fisiche “E. Pancini”, Complesso Universitario di Monte S. Angelo, Via Cintia ed. G, Napoli, 80126 Italy
[ac]Institute of Space Science - INFLPR Subsidiary, 409 Atomistilor Street, Magurele, Ilfov, 077125 Romania
[ad]University of Amsterdam, Institute of Physics/IHEF, PO Box 94216, Amsterdam, 1090 GE Netherlands
[ae]TNO, Technical Sciences, PO Box 155, Delft, 2600 AD Netherlands
[af]Università La Sapienza, Dipartimento di Fisica, Piazzale Aldo Moro 2, Roma, 00185 Italy
[ag]Università di Bologna, Dipartimento di Ingegneria dell’Energia Elettrica e dell’Informazione "Guglielmo Marconi", Via dell’Università 50, Cesena, 47521 Italia
[ah]Cadi Ayyad University, Physics Department, Faculty of Science Semlalia, Av. My Abdellah, P.O.B. 2390, Marrakech, 40000 Morocco
[ai]University of the Witwatersrand, School of Physics, Private Bag 3, Johannesburg, Wits 2050 South Africa
[aj]Università di Catania, Dipartimento di Fisica e Astronomia "Ettore Majorana", (INFN-CT) Via Santa Sofia 64, Catania, 95123 Italy
[ak]Princeton University, Department of Physics, Jadwin Hall, Princeton, New Jersey, 08544 USA
[al]INFN, Sezione di Bari, via Orabona, 4, Bari, 70125 Italy
[am]UCLouvain, Centre for Cosmology, Particle Physics and Phenomenology, Chemin du Cyclotron, 2, Louvain-la-Neuve, 1348 Belgium
[an]University of Granada, Department of Computer Engineering, Automation and Robotics / CITIC, 18071 Granada, Spain
[ao]Friedrich-Alexander-Universität Erlangen-Nürnberg (FAU), Erlangen Centre for Astroparticle Physics, Nikolaus-Fiebiger-Straße 2, 91058 Erlangen, Germany
[ap]NCSR Demokritos, Institute of Nuclear and Particle Physics, Ag. Paraskevi Attikis, Athens, 15310 Greece
[aq]University Mohammed I, Faculty of Sciences, BV Mohammed VI, B.P. 717, R.P. 60000 Oujda, Morocco
[ar]Western Sydney University, School of Science, Locked Bag 1797, Penrith, NSW 2751 Australia
[as]NIOZ (Royal Netherlands Institute for Sea Research), PO Box 59, Den Burg, Texel, 1790 AB, the Netherlands
[at]Leiden University, Leiden Institute of Physics, PO Box 9504, Leiden, 2300 RA Netherlands
[au]AGH University of Krakow, Al. Mickiewicza 30, 30-059 Krakow, Poland
[av]Tbilisi State University, Department of Physics, 3, Chavchavadze Ave., Tbilisi, 0179 Georgia
[aw]The University of Georgia, Institute of Physics, Kostava str. 77, Tbilisi, 0171 Georgia
[ax]Institut Universitaire de France, 1 rue Descartes, Paris, 75005 France
[ay]Max-Planck-Institut für Radioastronomie, Auf dem Hügel 69, 53121 Bonn, Germany
[az]University of Sharjah, Sharjah Academy for Astronomy, Space Sciences, and Technology, University Campus - POB 27272, Sharjah, - United Arab Emirates
[ba]University of Granada, Dpto. de Física Teórica y del Cosmos & C.A.F.P.E., 18071 Granada, Spain
[bb]School of Applied and Engineering Physics, Mohammed VI Polytechnic University, Ben Guerir, 43150, Morocco
[bc]University of Johannesburg, Department Physics, PO Box 524, Auckland Park, 2006 South Africa
[bd]Laboratoire Univers et Particules de Montpellier, Place Eugène Bataillon - CC 72, Montpellier Cédex 05, 34095 France
[be]Université de Haute Alsace, rue des Frères Lumière, 68093 Mulhouse Cedex, France
[bf]Université Badji Mokhtar, Département de Physique, Faculté des Sciences, Laboratoire de Physique des Rayonnements, B. P. 12, Annaba, 23000 Algeria
[bg]AstroCeNT, Nicolaus Copernicus Astronomical Center, Polish Academy of Sciences, Rektorska 4, Warsaw, 00-614 Poland
[bh]Charles University, Faculty of Mathematics and Physics, Ovocný trh 5, Prague, 116 36 Czech Republic
[bi]Harvard University, Black Hole Initiative, 20 Garden Street, Cambridge, MA 02138 USA

Acknowledgements

The authors acknowledge the financial support of: KM3NeT-INFRADEV2 project, funded by the European Union Horizon Europe Research and Innovation Programme under grant agreement No 101079679; Funds for Scientific Research (FRS-FNRS), Francqui foundation, BAEF foundation. Czech Science Foundation (GAČR 24-12702S); Agence Nationale de la Recherche (contract ANR-15-CE31-0020), Centre National de la Recherche Scientifique (CNRS), Commission Européenne (FEDER fund and Marie Curie Program), LabEx UnivEarthS (ANR-10-LABX-0023 and ANR-18-IDEX-0001), Paris Île-de-France Region, Normandy Region (Alpha, Blue-waves and Neptune), France, The Provence-Alpes-Côte d’Azur Delegation for Research and Innovation (DRARI), the Provence-Alpes-Côte d’Azur region, the Bouches-du-Rhône Departmental Council, the Metropolis of Aix-Marseille Provence and the City of Marseille through the

CPER 2021-2027 NEUMED project, The CNRS Institut National de Physique Nucléaire et de Physique des Particules (IN2P3); Shota Rustaveli National Science Foundation of Georgia (SRNSFG, FR-22-13708), Georgia; This research was funded by the European Union (ERC MuSES project No 101142396); The General Secretariat of Research and Innovation (GSRI), Greece; Istituto Nazionale di Fisica Nucleare (INFN) and Ministero dell'Università e della Ricerca (MUR), through PRIN 2022 program (Grant PANTHEON 2022E2J4RK, Next Generation EU) and PON R&I program (Avviso n. 424 del 28 febbraio 2018, Progetto PACK-PIR01 00021), Italy; IDMAR project Po-Fesr Sicilian Region az. 1.5.1; A. De Benedittis, W. Idrissi Ibnsalih, M. Bendahman, A. Nayerhoda, G. Papalashvili, I. C. Rea, A. Simonelli have been supported by the Italian Ministero dell'Università e della Ricerca (MUR), Progetto CIR01 00021 (Avviso n. 2595 del 24 dicembre 2019); KM3NeT4RR MUR Project National Recovery and Resilience Plan (NRRP), Mission 4 Component 2 Investment 3.1, Funded by the European Union – NextGenerationEU,CUP I57G21000040001, Concession Decree MUR No. n. Prot. 123 del 21/06/2022; Ministry of Higher Education, Scientific Research and Innovation, Morocco, and the Arab Fund for Economic and Social Development, Kuwait; Nederlandse organisatie voor Wetenschappelijk Onderzoek (NWO), the Netherlands; The grant "AstroCeNT: Particle Astrophysics Science and Technology Centre", carried out within the International Research Agendas programme of the Foundation for Polish Science financed by the European Union under the European Regional Development Fund; The program: "Excellence initiative-research university" for the AGH University in Krakow; The ARTIQ project: UMO-2021/01/2/ST6/00004 and ARTIQ/0004/2021; Ministry of Education and Scientific Research, Romania; Slovak Research and Development Agency under Contract No. APVV-22-0413; Ministry of Education, Research, Development and Youth of the Slovak Republic; MCIN for PID2021-124591NB-C41, -C42, -C43 and PDC2023-145913-I00 funded by MCIN/AEI/10.13039/501100011033 and by "ERDF A way of making Europe", for ASFAE/2022/014 and ASFAE/2022 /023 with funding from the EU NextGenerationEU (PRTR-C17.I01) and Generalitat Valenciana, for Grant AST22_6.2 with funding from Consejería de Universidad, Investigación e Innovación and Gobierno de España and European Union - NextGenerationEU, for CSIC-INFRA23013 and for CNS2023-144099, Generalitat Valenciana for CIDEGENT/2020/049, CIDEGENT/2021/23, CIDEIG/2023/20, ESGENT2024/24, CIPROM/2023/51, GRISOLIAP/2021/192 and INNVA1/2024/110 (IVACE+i), Spain; Khalifa University internal grants (ESIG-2023-008, RIG-2023-070 and RIG-2024-047), United Arab Emirates; The European Union's Horizon 2020 Research and Innovation Programme (ChETEC-INFRA - Project no. 101008324).

Views and opinions expressed are those of the author(s) only and do not necessarily reflect those of the European Union or the European Research Council. Neither the European Union nor the granting authority can be held responsible for them.

Full Authors List: The ANTARES Collaboration

A. Albert[a,b], S. Alves[c], M. André[d], M. Ardid[e], S. Ardid[e], J.-J. Aubert[f], J. Aublin[g], B. Baret[g], S. Basa[h], Y. Becherini[g], B. Belhorma[i], F. Benfenati[j,k], V. Bertin[f], S. Biagi[l], J. Boumaaza[m], M. Bouta[n], M.C. Bouwhuis[o], H. Brânzaş[p], R. Bruijn[o,q], J. Brunner[f], J. Busto[f], B. Caiffi[r], D. Calvo[c], S. Campion[s,t], A. Capone[s,t], F. Carenini[j,k], J. Carr[f], V. Carretero[c], T. Cartraud[g], S. Celli[s,t], L. Cerisy[f], M. Chabab[u], R. Cherkaoui El Moursli[m], T. Chiarusi[j], M. Circella[v], J.A.B. Coelho[g], A. Coleiro[g], R. Coniglione[l], P. Coyle[f], A. Creusot[g], A. F. Díaz[w], B. De Martino[f], C. Distefano[l], I. Di Palma[s,t], C. Donzaud[g,x], D. Dornic[f], D. Drouhin[a,b], T. Eberl[y], A. Eddymaoui[m], T. van Eeden[o], D. van Eijk[o], S. El Hedri[g], N. El Khayati[m], A. Enzenhöfer[f], P. Fermani[s,t], G. Ferrara[l], F. Filippini[j,k], L. Fusco[z], S. Gagliardini[s,t], J. García-Méndez[e], C. Gatius Oliver[o], P. Gay[aa,g], N. Geißelbrecht[y], H. Glotin[ab], R. Gozzini[c], R. Gracia Ruiz[y], K. Graf[y], C. Guidi[r,ac], L. Haegel[g], H. van Haren[ad], A.J. Heijboer[o], Y. Hello[ae], L. Hennig[y], J.J. Hernández-Rey[c], J. Hößl[y], F. Huang[f], G. Illuminati[j,k], B. Jisse-Jung[o], M. de Jong[o,af], P. de Jong[o,q], M. Kadler[ag], O. Kalekin[y], U. Katz[y], A. Kouchner[g], I. Kreykenbohm[ah], V. Kulikovskiy[r], R. Lahmann[y], M. Lamoureux[g], A. Lazo[c], D. Lefèvre[ai], E. Leonora[aj], G. Levi[j,k], S. Le Stum[f], S. Loucatos[ak,g], J. Manczak[c], M. Marcelin[h], M. Marconi[r,ac], A. Margiotta[j,k], A. Marinelli[al,am], J.A. Martínez-Mora[e], P. Migliozzi[al], A. Moussa[n], R. Muller[o], S. Navas[an], E. Nezri[h], B. Ó Fearraigh[o], E. Oukacha[g], A.M. Păun[p], G.E. Păvălaş[p], S. Peña-Martínez[g], M. Perrin-Terrin[f], P. Piattelli[l], C. Poirè[z], V. Popa[p], T. Pradier[a], N. Randazzo[aj], D. Real[c], G. Riccobene[l], A. Romanov[r,ac], A. Sánchez Losa[c], A. Saina[c], F. Salesa Greus[c], D. F. E. Samtleben[o,af], M. Sanguineti[r,ac], P. Sapienza[l], F. Schüssler[ak], J. Seneca[o], M. Spurio[j,k], Th. Stolarczyk[ak], M. Taiuti[r,ac], Y. Tayalati[m], B. Vallage[ak,g], G. Vannoye[f], V. Van Elewyck[g,ao], S. Viola[l], D. Vivolo[ap,al], J. Wilms[ah], S. Zavatarelli[r], A. Zegarelli[s,t], J.D. Zornoza[c], J. Zúñiga[c].

[a]Université de Strasbourg, CNRS, IPHC UMR 7178, F-67000 Strasbourg, France

[b] Université de Haute Alsace, F-68100 Mulhouse, France

[c]IFIC - Instituto de Física Corpuscular (CSIC - Universitat de València) c/ Catedrático José Beltrán, 2 E-46980 Paterna, Valencia, Spain

[d]Technical University of Catalonia, Laboratory of Applied Bioacoustics, Rambla Exposició, 08800 Vilanova i la Geltrú, Barcelona, Spain

[e]Institut d'Investigació per a la Gestió Integrada de les Zones Costaneres (IGIC) - Universitat Politècnica de València. C/ Paranimf 1, 46730 Gandia, Spain

[f]Aix Marseille Univ, CNRS/IN2P3, CPPM, Marseille, France

[g]Université Paris Cité, CNRS, Astroparticule et Cosmologie, F-75013 Paris, France

[h]Aix Marseille Univ, CNRS, CNES, LAM, Marseille, France

[i]National Center for Energy Sciences and Nuclear Techniques, B.P.1382, R. P.10001 Rabat, Morocco

[j]INFN - Sezione di Bologna, Viale Berti-Pichat 6/2, 40127 Bologna, Italy

[k]Dipartimento di Fisica e Astronomia dell'Università di Bologna, Viale Berti-Pichat 6/2, 40127, Bologna, Italy

[l]INFN - Laboratori Nazionali del Sud (LNS), Via S. Sofia 62, 95123 Catania, Italy

[m]University Mohammed V in Rabat, Faculty of Sciences, 4 av. Ibn Battouta, B.P. 1014, R.P. 10000 Rabat, Morocco

[n]University Mohammed I, Laboratory of Physics of Matter and Radiations, B.P.717, Oujda 6000, Morocco

[o]Nikhef, Science Park, Amsterdam, The Netherlands
[p]Institute of Space Science - INFLPR subsidiary, 409 Atomistilor Street, Măgurele, Ilfov, 077125 Romania
[q]Universiteit van Amsterdam, Instituut voor Hoge-Energie Fysica, Science Park 105, 1098 XG Amsterdam, The Netherlands
[r]INFN - Sezione di Genova, Via Dodecaneso 33, 16146 Genova, Italy
[s]INFN - Sezione di Roma, P.le Aldo Moro 2, 00185 Roma, Italy
[t]Dipartimento di Fisica dell'Università La Sapienza, P.le Aldo Moro 2, 00185 Roma, Italy
[u]LPHEA, Faculty of Science - Semlali, Cadi Ayyad University, P.O.B. 2390, Marrakech, Morocco.
[v]INFN - Sezione di Bari, Via E. Orabona 4, 70126 Bari, Italy
[w]Department of Computer Architecture and Technology/CITIC, University of Granada, 18071 Granada, Spain
[x]Université Paris-Sud, 91405 Orsay Cedex, France
[y]Friedrich-Alexander-Universität Erlangen-Nürnberg, Erlangen Centre for Astroparticle Physics, Erwin-Rommel-Str. 1, 91058 Erlangen, Germany
[z]Università di Salerno e INFN Gruppo Collegato di Salerno, Dipartimento di Fisica, Via Giovanni Paolo II 132, Fisciano, 84084 Italy
[aa]Laboratoire de Physique Corpusculaire, Clermont Université, Université Blaise Pascal, CNRS/IN2P3, BP 10448, F-63000 Clermont-Ferrand, France
[ab]LIS, UMR Université de Toulon, Aix Marseille Université, CNRS, 83041 Toulon, France
[ac]Dipartimento di Fisica dell'Università, Via Dodecaneso 33, 16146 Genova, Italy
[ad]Royal Netherlands Institute for Sea Research (NIOZ), Landsdiep 4, 1797 SZ 't Horntje (Texel), the Netherlands
[ae]Géoazur, UCA, CNRS, IRD, Observatoire de la Côte d'Azur, Sophia Antipolis, France
[af]Huygens-Kamerlingh Onnes Laboratorium, Universiteit Leiden, The Netherlands
[ag]Institut für Theoretische Physik und Astrophysik, Universität Würzburg, Emil-Fischer Str. 31, 97074 Würzburg, Germany
[ah]Dr. Remeis-Sternwarte and ECAP, Friedrich-Alexander-Universität Erlangen-Nürnberg, Sternwartstr. 7, 96049 Bamberg, Germany
[ai]Mediterranean Institute of Oceanography (MIO), Aix-Marseille University, 13288, Marseille, Cedex 9, France; Université du Sud Toulon-Var, CNRS-INSU/IRD UM 110, 83957, La Garde Cedex, France
[aj]INFN - Sezione di Catania, Via S. Sofia 64, 95123 Catania, Italy
[ak]IRFU, CEA, Université Paris-Saclay, F-91191 Gif-sur-Yvette, France
[al]INFN - Sezione di Napoli, Via Cintia 80126 Napoli, Italy
[am]Dipartimento di Fisica dell'Università Federico II di Napoli, Via Cintia 80126, Napoli, Italy
[an]Dpto. de Física Teórica y del Cosmos & C.A.F.P.E., University of Granada, 18071 Granada, Spain
[ao]Institut Universitaire de France, 75005 Paris, France
[ap]Dipartimento di Matematica e Fisica dell'Università della Campania L. Vanvitelli, Via A. Lincoln, 81100, Caserta, Italy

Acknowledgements

The authors acknowledge the financial support of the funding agencies: Centre National de la Recherche Scientifique (CNRS), Commissariat à l'énergie atomique et aux énergies alternatives (CEA), Commission Européenne (FEDER fund and Marie Curie Program), LabEx UnivEarthS (ANR-10-LABX-0023 and ANR-18-IDEX-0001), Région Alsace (contrat CPER), Région Provence-Alpes-Côte d'Azur, Département du Var and Ville de La Seyne-sur-Mer, France; Bundesministerium für Bildung und Forschung (BMBF), Germany; Istituto Nazionale di Fisica Nucleare (INFN), Italy; Nederlandse organisatie voor Wetenschappelijk Onderzoek (NWO), the Netherlands; Ministry of Education and Scientific Research, Romania; MCIN for PID2021-124591NB-C41, -C42, -C43 and PDC2023-145913-I00 funded by MCIN/AEI/10.13039/501100011033 and by "ERDF A way of making Europe", for ASFAE/2022/014 and ASFAE/2022 /023 with funding from the EU NextGenerationEU (PRTR-C17.I01) and Generalitat Valenciana, for Grant AST22_6.2 with funding from Consejería de Universidad, Investigación e Innovación and Gobierno de España and European Union - NextGenerationEU, for CSIC-INFRA23013 and for CNS2023-144099, Generalitat Valenciana for CIDEGENT/2020/049, CIDEGENT/2021/23, CIDEIG/2023/20, ESGENT2024/24, CIPROM/2023/51, GRISOLIAP/2021/192 and INNVA1/2024/110 (IVACE+i), Spain; Ministry of Higher Education, Scientific Research and Innovation, Morocco, and the Arab Fund for Economic and Social Development, Kuwait. We also acknowledge the technical support of Ifremer, AIM and Foselev Marine for the sea operation and the CC-IN2P3 for the computing facilities.